W. I., and Hill, C. P. (1996) *Cell* **87,** 1285–1294
10. Gross, I., Hohenberg, H., Huckhagel, C., and Krausslich, H. G. (1998) *J. Virol.* **72,** 4798–4810
11. Turner, B. G., and Summers, M. F. (1999) *J. Mol. Biol.* **285,** 1–32
12. Mimoto, T., Imai, J., Kisanuki, S., Enomoto, H., Hattori, N., Akaji, K., and Kiso, Y. (1992) *Chem. Pharm. Bull.* **40,** 2251–2253
13. Kageyama, S., Mimoto, T., Murakawa, Y., Nomizu, M., Ford, H., Shirasaka, T., Gulnik, S., Erickson, J., Takada, K., Hayashi, H., Broder, S., Kiso, Y., and Mitsuya, H. (1993) *Antimicrob. Agents Chemother.* **37,** 810–817
14. Yoshimura, K., Kato, R., Yusa, K., Kavlick, M. F., Maroun, V., Nguyen, A., Mimoto, T., Ueno, T., Shintani, M., Falloon, J., Masur, H., Hayashi, H., Erickson, J., and Mitsuya, H. (1999) *Proc. Natl. Acad. Sci. U. S. A.* **96,** 8675–8680
15. Ghosh, A. K., Kincaid, J. F., Cho, W., Walters, D. E., Krishnan, K., Hussain, K. A., Koo, Y., Cho, H., Rudall, C., Holland, L., and Buthod, J. (1998) *Bioorg. Med. Chem. Lett.* **8,** 687–690
16. Yoshimura, K., Kato, R., Kavlick, M. F., Nguyen, A., Maroun, V., Maeda, K., Hussain, K. A., Ghosh, A. K., Gulnik, S. V., Erickson, J. W., and Mitsuya, H. (2002) *J. Virol.* **76,** 1349–1358
17. Kimpton, J., and Emerman, M. (1992) *J. Virol.* **66,** 2232–2239
18. Kosalaraksa, P., Kavlick, M. F., Maroun, V., Le, R., and Mitsuya, H. (1999) *J. Virol.* **73,** 5356–5363
19. Tamiya, S., Mardy, S., Kavlick, M. F., Yoshimura, K., and Mitsuya, H. (2004) *J. Virol.* **78,** 12030–12040
20. Kaminski, G. A., Friesner, R. A., Tirado-Rives, J., and Jorgensen, W. J. (2001) *J. Phys. Chem.* **105,** 6474–6487
21. Still, W. C., Tempczyk, A., Hawley, R. C., and Hendrickson, T. (1990) *J. Am. Chem. Soc.* **112,** 6127–6129
22. Kuiken, C., Foley, B., Hahn, B., Marx, P., McCutchan, F., Mellors, J. W., Mullins, J., Wolinsky, S., and Korber, B. (2000) in *Human Retroviruses and AIDS* (Bradac, J., ed) pp. 201–298, Los Alamos National Laboratory, Los Alamos, NM
23. Yin, L., Braaten, D., and Luban, J. (1998) *J. Virol.* **72,** 6430–6436
24. Braaten, D., Aberham, C., Franke, E. K., Yin, L., Phares, W., and Luban, J. (1996) *J. Virol.* **70,** 5170–5176
25. Cornelissen, M., van den Burg, R., Zorgdrager, F., Lukashov, V., and Goudsmit, J. (1997) *J. Virol.* **71,** 6348–6358
26. Quinones-Mateu, M. E., Albright, J. L., Mas, A., Soriano, V., and Arts, E. J. (1998) *J. Virol.* **72,** 9002–9015
27. Colson, P., Henry, M., Tourres, C., Lozachmeur, D., Gallais, H., Gastaut, J. A., Moreay, J., and Tamalet, C. (2004) *J. Clin. Microbiol.* **42,** 570–577
28. Li, Q., Moutiez, M., Charbonnier, J. B., Vaudry, K., Menez, A., Quemeneur, E., and Dugave, C. (2000) *J. Med. Chem.* **43,** 1770–1779
29. Yoo, S., Myszka, D. G., Yeh, C., McMurray, M., Hill, C. P., and Sundquist, W. I. (1997) *J. Mol. Biol.* **269,** 780–795
30. Thali, M., Bukovsky, A., Kondo, E., Rosenwirth, B., Walsh, C. T., and Sodroski, J. (1994) *Nature* **372,** 363–365
31. Ackerson, B., Rey, O., Canon, J., and Krogstad, P. (1998) *J. Virol.* **72,** 303–308
32. Stremlau, M., Owens, C. M., Perron, M. J., Kiessling, M., Autissier, P., and Sodroski, J. (2004) *Nature* **427,** 848–853
33. Owens, C. M., Yang, P. C., Göttlinger, H., and Sodroski, J. (2003) *J. Virol.* **77,** 726–731
34. Owens, C. M., Song, B., Perron, M. J., Yang, P. C., Stremlau, M., and Sodroski, J. (2004) *J. Virol.* **78,** 5423–5437
35. Kootstra, N. A., Münk, C., Tonnu, N., Landau, N. R., and Verma, I. M. (2003) *Proc. Natl. Acad. Sci. U. S. A.* **100,** 1298–1303
36. Towers, G. J., Hatziioannou, T., Cowan, S., Goff, S. P., Luban, J., and Bieniasz, P. D. (2003) *Nat. Med.* **9,** 1138–1143

JBC Papers in Press. Published on February 13, 2006 as Manuscript M512688200
The latest version is at http://www.jbc.org/cgi/doi/10.1074/jbc.M512688200

STRUCTURAL AND MOLECULAR INTERACTIONS OF CCR5 INHIBITORS WITH CCR5

Kenji Maeda[1,2,3], Debananda Das[3], Hiromi Ogata-Aoki[1,2], Hirotomo Nakata[1,2], Toshikazu Miyakawa[2], Yasushi Tojo[1,2], Rachael Norman[3], Yoshikazu Takaoka[4], Jianping Ding[5], Eddy Arnold[5], and Hiroaki Mitsuya[1,2,3]

From [1]Department of Hematology and [2]Department of Infectious Diseases, Kumamoto University Graduate School of Medical and Pharmaceutical Sciences, Kumamoto 860-8556, Japan; [3]Experimental Retrovirology Section, HIV and AIDS Malignancy Branch, National Cancer Institute, Bethesda, MD 20892, USA; [4]Minase Research Institute, Ono Pharmaceutical Co. Ltd., Osaka 618-8585; [5]Center for Advanced Biotechnology and Medicine, and Chemistry and Chemical Biology Department, Rutgers University, Piscataway, NJ 08854, USA.

Running Title: Interactions of CCR5 inhibitors with CCR5

Address correspondence to: Hiroaki Mitsuya, Department of Infectious Diseases, Kumamoto University Graduate School of Medical and Pharmaceutical Science, 1-1-1 Honjo, Kumamoto 860-8556, Japan, Tel. (+81) 96-373-5156; Fax. (+81) 96-363-5265; E-Mail: hmitsuya@helix.nih.gov

We have characterized the structural and molecular interactions of CC-chemokine receptor 5 (CCR5) with three CCR5 inhibitors active against R5 human immunodeficiency virus type 1 (HIV-1) including a potent *in vitro* and *in vivo* CCR5 inhibitor aplaviroc (AVC). The data obtained with saturation binding assays and structural analyses delineated the key interactions responsible for the binding of CCR5 inhibitors with CCR5 and illustrated that their binding site is located in a predominantly lipophilic pocket in the interface of extracellular loops (ECLs) and within the upper transmembrane (TM) domain of CCR5. Mutations in the CCR5 binding sites of AVC decreased gp120 binding to CCR5 and the susceptibility to HIV-1 infection, while mutations in TM4 and TM5 that also decreased gp120 binding and HIV-1 infectivity had less effects on the binding of CC-chemokines, suggesting that CCR5 inhibition targeting appropriate regions might render the inhibition highly HIV-1-specific while preserving the CC chemokine-CCR5 interactions. The present data delineating residue-by-residue interactions of CCR5 with CCR5 inhibitors should not only help design more potent and more HIV-1-specific CCR5 inhibitors, but also give new insights into the dynamics of CC-chemokine-CCR5 interactions and the mechanisms of CCR5 involvement in the process of cellular entry of HIV-1.

Highly active antiretroviral therapy (HAART) has brought about a major impact on the acquired immunodeficiency syndrome (AIDS) epidemics in industrially advanced nations (1,2), however, eradication of HIV-1 appears to be currently impossible mainly due to the viral reservoirs remaining in blood and infected tissues (3). Successful antiviral drugs, in theory, exert their virus-specific effects by interacting with viral components such as viral genes or their transcripts without disturbing cellular metabolisms or functions (2). However, at present, no antiretroviral drugs or agents have been demonstrated to be completely specific for HIV-1 and devoid of toxicity or side effects in the therapy of AIDS (4). Limitations of antiviral therapy of AIDS are exacerbated by complicated regimens, emergence of drug resistant HIV-1 variants (1), and a number of inherent adverse effects (5).

Thus, identification of new antiretroviral drugs which have unique mechanisms of action and produce no or least minimal side effects remains an important therapeutic objective

(2,4). CCR5 is a member of G protein-coupled, seven- transmembrane segment receptors (GPCRs), which comprise the largest superfamily of proteins in the body (6). In 1996, it was revealed that CCR5 serves as one of the two essential co-receptors for HIV-1 entry to human $CD4^+$ cells, thereby serving as an attractive target for possible intervention of HIV-1 infection (7-10). Aplaviroc (AVC; AK602/ONO4128/873140; Fig. 1), a novel spirodiketopiperazine derivative, represents a CCR5 inhibitor which specifically binds to human CCR5 with a high affinity, greatly blocks HIV-1-gp120/CCR5 binding, and exerts potent activity against a wide spectrum of laboratory and primary R5-HIV-1 isolates including multi-drug resistant $HIV\text{-}1_{MDR}$ (IC_{50} values of 0.2-0.6 nM) (11). AVC, despite its much greater anti-HIV-1 activity than other previously published CCR5 inhibitors including TAK-779 and SCH-C (Fig. 1), preserves RANTES and MIP-1β binding to $CCR5^+$ cells and their functions, while TAK-779 and SCH-C fully block the CC-chemokines/CCR5 interactions (11). AVC reportedly has an extensive and prolonged CCR5 occupancy as examined in phytohemagglutinin-activated peripheral blood mononuclear cells ($T_{1/2}$ ~9 hr) (12) and in circulating lymphocytes in HIV-1-negative and HIV-1-positive individuals ($T_{1/2}$ of 69-152 hr depending on different AVC doses)(S. Sparks *et al.*, 12th Conference on Retroviruses and Opportunistic Infections, abstr. 77, 2005). In a randomized, placebo-controlled short-term monotherapy trial in patients with AIDS including those who were drug-experienced, AVC demonstrated potent antiretroviral activity and brought about significant reduction in HIV-1 viremia (by ~ 1.7 log) in AIDS patients (J. Lalezari *et al.*, 44th Interscience Conference on Antimicrobial Agents and Chemotherapy, abstr. H-1137b, 2004).

In the present study, we examined the profile of binding to and interactions with CCR5 of three CCR5 inhibitors, AVC, SCH-C and TAK-779. We also conducted structural analyses of the interactions of CCR5 inhibitors with CCR5, using homology modeling, robust structure refinement, and docking. Notably, the molecular modeling analyses were combined and fine-tuned with the results of the saturation binding assay using a panel of mutant CCR5-expressing cells and ^{3}H-CCR5 inhibitors and the resultant configurations and orientations of inhibitors docked within the hydrophobic cavity of CCR5 yielded structure-activity predictions and interpretations consistent with the observed experimental data. The present approach of combining the site-directed mutagenesis-based data and molecular modeling should represent a valuable strategy for gaining structural insights for membrane-bound proteins for which X-ray crystal structures are not as yet available. The present data delineating residue-by-residue interactions of CCR5 with CCR5 inhibitors should not only help design more potent and more HIV-1-specific CCR5 inhibitors, but also give new insights into the dynamics of CC-chemokine-CCR5 interactions and the mechanisms of CCR5 involvement in the process of cellular entry of HIV-1.

Experimental Procedures

Reagents - A CCR5 inhibitor, aplaviroc (AVC), was designed and synthesized as previously published (11). Two other CCR5 inhibitors, TAK-779 and SCH-351125 (SCH-C) were synthesized based on the previously published structures (13,14)(Fig. 1). These three CCR5 inhibitors were tritiated by reductive amination with sodium triacetoxyborotritide (15), methylation with [^{3}H]methyliodide, and/or heterogeneous catalytic exchange with tritium gas (16). Two ^{125}I-labeled chemokines [macrophage inflammatory protein-1α (MIP-1α) and regulated upon activation, normal T cell expressed and secreted (RANTES)] were purchased from Amersham Pharmacia Biotech (Little Chalfont, UK) and ^{125}I-labeled macrophage inflammatory protein-1β (MIP-1β) was purchased from PerkinElmer Life Sciences, Inc. (Boston, MA). Their corresponding unlabeled chemokines were purchased from PeproTech Inc. (Rocky Hill, NJ). Recombinant $HIV\text{-}1_{YU2}$ gp120 (rgp120) and human soluble CD4 (sCD4) were purchased from Immuno Diagnostics, Inc. (Woburn, MA).

Cells and Viruses - The Chinese hamster ovary (CHO) cells overexpressing CCR5 (17) were maintained in Ham's F-12 medium (GIBCO-BRL, Rockville, MD) supplemented with 10% fetal calf serum (FCS: JRH Biosciences, Lenaza, KS) and 50 U/ml penicillin and 50 μg/ml streptomycin in the presence of 5 μg/ml blasticidin S hydrochloride.

The HeLa-CD4-LTR-β-gal indicator cell line expressing human CCR5 [$CCR5^+$MAGI (multinuclear activation of galactosidase indicator) cells] (18) was a kind gift from Dr. Yosuke Maeda, Kumamoto University Graduate School of Medical and Pharmaceutical Sciences, Japan. $CCR5^+$MAGI cells were maintained in Dulbecco's modified Eagle's medium (DMEM) supplemented with 10% FCS, 200 μg/ml G418, 100 μg/ml hygromycin B, and 100 μg/ml zeomycin. The U373-MAGI cell line was obtained from the AIDS Research and Reference Reagent Program, NIAID, National Institutes of Health (Bethesda, MD). U373-MAGI cells were maintained in DMEM supplemented with 10% FCS, 200 μg/ml G418, and 100 μg/ml hygromycin B. An R5-HIV-1 strain, $HIV\text{-}1_{BaL}$, was employed for the determination of the susceptibility of mutant CCR5 ($CCR5_{MT}$)-expressing cells to the infectivity of HIV-1.

Generation of wild type and $CCR5_{MT}$-overexpressing cells - A mammalian expression vector pZeoSV2 (Invitrogen, Carlsbad, CA) carrying human wild type CCR5 ($CCR5_{WT}$) gene (pZeoSV-CCR5) (18) was a kind gift from Dr. Yosuke Maeda. A variety of plasmids carrying a mutant CCR5-encoding gene were generated using the site-directed mutagenesis technique employing QuickChange site-directed mutagenesis kit (Stratagene, La Jolla, CA) as described by the manufacturer. Mutations introduced into the CCR5 gene were introduced through: (i) substitution of an amino acid(s) or (ii) deletion of an amino acid(s) at selected amino acid positions of CCR5. A mutation from Gly to Arg at position 163, where the corresponding amino acid in simian CCR5 is Arg, was also introduced. This G163R substitution has been reported to reduce the binding of R5-HIV-1-gp120 to human CCR5 and the susceptibility to HIV-1 (19). All these plasmids were confirmed to contain only desired mutation(s) by nucleotide sequencing.

CHO cells (or U373-MAGI cells) were transfected with a plasmid containing $CCR5_{WT}$-encoding gene or a plasmid carrying a $CCR5_{MT}$-encoding gene using Lipofectamine (Gibco BRL); the transfectants were magnetically sorted, following treatment with an anti-CCR5 monoclonal antibody (2D7 or 3A9; BD PharMingen, San Diego, CA), using Dynabeads M-450 coupled to goat anti-mouse IgG (Dynal A.S. Oslo, Norway); and the cells were cloned using the limiting dilution technique.

Determination of CCR5 expression levels in CHO and U373-MAGI cells - CCR5 expression levels of various clones described above were determined using three indicators: (i) maximal amounts of ^{3}H-AVC bound to cells (B_{max}); (ii) mean florescence intensity (MFI) values when stained with monoclonal antibody (mAb) 3A9; and (iii) MFI values when stained with mAb 2D7. The antigenic epitope for 2D7 is located distant from that for 3A9 (20) and 3A9 does not compete with AVC binding to CCR5 (data not shown). The expression levels were expressed as % control ($CCR5_{WT}$-expressing cells as control), and the highest value obtained was chosen as the estimated CCR5 expression level. There were no clones which had low values in all three indicators, thus sustaining that the current method used for CCR5 expression levels was thought to be legitimate. CD4 and CCR5 expression levels were also determined using the quantitative fluorescence-activated cell sorting (QFACS) assay system (Quantum Simply Cellular Kit; Sigma, Saint Louis, MO) using 3A9 and 2D7 (12). For the HIV-1 susceptibility assay, U373-MAGI clones which expressed CD4 molecules ranging 10-25 x 10^4 antigen-binding sites (ABS) were selected. $CCR5_{MT}$-expressing CHO cells were maintained in Ham's F-12 medium containing 10% FCS and 100 μg/ml zeomycin. $CCR5_{WT}$- and $CCR5_{MT}$-expressing U373-MAGI cells were cultured in a DMEM supplemented with 10% FCS, 200 μg/ml G418, 100 μg/ml hygromycin B, and 100 μg/ml zeomycin.

Saturation binding assay using ^{3}H-labeled CCR5 inhibitors - Saturation binding assay using ^{3}H-labeled CCR5 inhibitors was conducted and the K_D (dissociation constant) values of CCR5 inhibitors in $CCR5_{WT}$-, or $CCR5_{MT}$-expressing CHO cells were calculated as previously described (11).

Radiolabeled inhibitor binding/competition studies – $CCR5_{WT}$-expressing cells (1.5×10^5) were plated onto 48-well microculture plates, incubated for 24

hrs, rinsed, exposed to ^{3}H-AVC, ^{3}H-SCH-C, or ^{3}H-TAK-779 for 15 min at room temperature, subsequently exposed to various concentrations of unlabelled CCR5 inhibitors, incubated for 30 min, thoroughly washed, lysed, and the radioactivity in the lysates was counted. All experiments were performed in duplicate. The amounts of each ^{3}H-labeled CCR5 inhibitor bound to the cells are shown as mean % control values. Standard deviation (SD) values are indicated with the vertical lines. To obtain control values, the experiment was also performed without the addition of unlabelled CCR5 inhibitors.

Determination of CC-chemokine- and HIV-1 gp120-binding affinity to $CCR5_{WT}$ and $CCR5_{MT}$ - Binding profiles of chemokines to $CCR5_{WT}$- or $CCR5_{MT}$-expressing cells were determined using ^{125}I-labeled chemokines as previously reported (11) with minor modifications. In brief, $CCR5_{WT}$- or $CCR5_{MT}$-expressing cells (1.5×10^{5}) were plated onto 48-well microculture plates, incubated for 24 hrs, rinsed, exposed to 5 nM ^{125}I-MIP-1α, ^{125}I-MIP-1β, or ^{125}I-RANTES at room temperature for 1 hr, thoroughly washed with PBS, lysed with 0.5 ml of 1N NaOH, and the radioactivity in the lysates was counted. The non-specific binding of the labeled chemokine to the cells was determined based on the radioactivity detected in the wells plated with the same number of CCR5-negative CHO (CHO-K1) cells exposed to an equal amount of ^{125}I-labeled chemokine. Determination of the binding profiles of HIV-1-rgp120 to $CCR5_{WT}$ or $CCR5_{MT}$ was also conducted. Briefly, $CCR5^{+}$CHO cells were exposed to rgp120 (5 μg/ml) and sCD4 [5 μg/ml: biotinylated using EZ-link sulfo-NHS-SS-biotin (Pierce, Rockford, IL)] for 1 hr at 37°C. Cells were washed and the binding of the rgp120-sCD4 complex to $CCR5^{+}$CHO cells was determined using phycoerythrin-conjugated streptavidin (SA-PE: BD PharMingen). Non-specific binding was determined based on the MFI of SA-PE with sCD4 but without rgp120. Since CCR5 expression levels vary among CCR5 clones, the % binding (occupancy) values for ^{125}I-chemokines and rgp120 were normalized using the following formula: % binding (occupancy) = 100 x [amount of ^{125}I-chemokine or rgp120 bound to $CCR5_{MT}$/amount of ^{125}I-chemokine or rgp120 bound to $CCR5_{WT}$]x[number of $CCR5_{WT}$ /number of $CCR5_{MT}$], where numbers of $CCR5_{WT}$ and $CCR5_{MT}$ are expressed as B_{max} (cpm) or MFI values as described above.

Determination of HIV-1 susceptibility of $CCR5_{WT}$- and $CCR5_{MT}$-expressing cells - The susceptibility of $CCR5_{WT}$- and $CCR5_{MT}$-expressing cells to the infection by an R5-HIV-1 strain, $HIV\text{-}1_{BaL}$, was determined as previously described (22). In brief, target cells ($CCR5_{WT}$- or $CCR5_{MT}$-expressing U373-MAGI cells; 10^{4}/well) were plated onto 96-well flat microtiter culture plates, inoculated with 100 $TCID_{50}$ of $HIV\text{-}1_{BaL}$ on the following day, cultured for 48-72 hrs, stained with 400 μg/ml of X-gal, and all blue cells were counted. All experiments were performed in triplicate. For testing each of $CCR5_{MT}$-expressing cell preparations, multiple (5 to 13) clones were examined. In each set of experiments, $CCR5_{WT}$-clone #1 was included and served as a standard. Percent infection in $CCR5_{WT}$- and $CCR5_{MT}$-expressing cells was determined using the following formula: % Infection = 100 x (mean blue cell number in a well)/(mean blue cell number in a well of $CCR5_{WT}$-clone #1).

Structural modeling of the interactions of CCR5 inhibitors with wild-type and mutant CCR5 species - An initial structural model of CCR5 was defined with homology modeling using the crystal structure of bovine rhodopsin as a template (23). This resulted in the initial placement of the helices and side chains. The CCR5-inhibitor complex structures were defined with an iterative optimization of CCR5 and inhibitor structures in the presence of each other, using software tools from Schrödinger (Schrödinger, LLC, New York, NY 2005), as described below. The conformational flexibility of both CCR5 and the inhibitors were taken into account. The molecular structures of AVC, SCH-C, and TAK-779 were obtained by minimization using the MMFF94 force field (24). For each minimized inhibitor configuration, a set of low energy structures was generated by performing a Monte Carlo sampling of their conformations. Thus obtained structures were used as starting structures for docking calculations where their conformations were further refined.

The protonation states of CCR5 residues were assigned, and residues more than 20 Å from the active site were neutralized. In an attempt to place an inhibitor within CCR5, initially the active site was artificially enlarged by mutating Tyr108, Cys178, Glu283, and Met287 to Ala. The van der Waals radii of inhibitor atoms were scaled by a factor of 0.70 to reduce steric clashes and docked into CCR5. After obtaining an initial set of CCR5-inhibitor complexes, residues 108, 178, 283, and 287 were mutated back from Ala to their original states. CCR5 atoms within 15 Å of an initially placed inhibitor were subsequently refined. It was achieved by using the rotamer library of Xiang and Honig (25) and optimizing each side chain one at a time holding all other side chains fixed. After convergence, all side chains were simultaneously energy minimized using the OPLS-AA force field (26) to remove any remaining clashes. The inhibitors were docked again and scored to estimate their relative affinity. The docked complexes with higher scores were visually examined along with the mutational data to select the best possible CCR5-inhibitor complex.

Mutated CCR5 structures were defined using wild type CCR5 structure and optimized using the OPLS2003 force field. Charges were taken from the force field. The minimization was carried out until the gradient was below 0.2 kJ/Å-mol. Resulting minimized structures were used as starting structures for obtaining docked complexes of mutated CCR5 with inhibitors using the protocol described above. Visualization, structural refinement, and docking were performed using Maestro 7.0, MacroModel 9.0, Prime 1.2, Glide 3.5, and IFD script from Schrödinger, LLC (New York, NY 2005). The extra-precision mode of Glide, which has higher penalty for unfavorable and unphysical interactions, was used (27). Computations were carried out on a multiprocessor SGI Origin 3400 computer platform.

A probe radius of 1.4 Å with Connolly surfaces generated was used to define binding site cavities using the method of Exner *et al.* (28) as implemented in the MOLCAD tool in Sybyl 7.0 (Tripos, Inc., St. Louis, MO). Lipophilic potential was mapped onto the cavities using parameters from Viswanadhan *et al.* (29).

RESULTS

Site-directed mutagenesis of CCR5 and binding affinity of CCR5 inhibitors – We have previously reported (11) that AVC competitively blocked the binding of a monoclonal antibody, 45531, which is known to be specific against the C-terminal half (or domain B) of the second extracellular loop (ECL2B) of CCR5 (21) while AVC failed to block or only partially blocked the binding of two other monoclonal antibodies, 2D7 and 45523, specific for CCR5 but not for its ECL2B. When we examined three additional monoclonal antibodies, 3A9 and 45502 (both specific for NH_2-terminus) and 45549 (multi-domain-reactive)(20,21), none of these antibodies were replaced by AVC (data not shown). These data suggest that the potent inhibitory activity of AVC against R5 HIV-1 infection stems from its binding to ECL2B and/or its vicinity with high affinity.

In an attempt to delineate the CCR5 binding profile of the three CCR5 inhibitors, we generated a variety of CCR5 mutant-overexpressing ($CCR5_{MT}$) CHO cells and determined the K_D values of each inhibitor to mutant CCR5 species using the saturation binding assay with tritiated inhibitors. When we determined the K_D value of AVC with respect to a CCR5 mutant carrying an Asp to Ala substitution at position 11 of the amino-terminus domain ($CCR5_{D11A}$), the value was 3.0 nM, virtually identical to the K_D value with wild-type CCR5 ($CCR5_{WT}$; Table 1), indicating that the D11A substitution did not affect the binding of AVC to CCR5. The K_D value of AVC with respect to $CCR5_{Y37A}$ was moderately greater with 7.9 nM (2.7-fold compared to the K_D value with regard to $CCR5_{WT}$). On the other hand, those of TAK-779 and SCH-C to $CCR5_{Y37A}$ were 98.9 nM (3.3-fold compared to the K_D with regard to $CCR5_{WT}$) and >200 nM (>12.5-fold), respectively, in agreement with the previous reports in which both TAK-779 and SCH-C apparently failed to bind, probably explaining that these inhibitors failed to block HIV-1 infection of $CCR5_{Y37A}$-expressing cells (30,31). These data suggest that the binding of TAK-779 and SCH-C to $CCR5_{WT}$ is more dependent on interactions with Tyr37 than that of AVC. We also generated a series of CCR5-overexpressing CHO cells carrying a mutation(s) at a selected amino acid position(s).

As shown in Table 1, the mutations which substantially (more than 3-fold compared to AVC binding to $CCR5_{WT}$) affected the K_D values of AVC were as follows: Y108A and F113A in the third transmembrane domain (TM3) of CCR5; R168A and S180E in ECL2; K191R and K191N of the interface of ECL2B and TM5; K197A and I198A of TM5; Y251A of TM6; and M287E of TM7. The mutations which greatly diminished the binding of AVC (values of >200 nM) to CCR5 were as follows: G163R, C178A, WKNF190del, K191A, and E283A. It is worthwhile to interject that Lys191 in ECL2 is reported to be critical for the binding of RANTES, MIP-1α, and MIP-1β to CCR5 (32,33), while Cys178 is presumed to form a disulfide bond with Cys101 of ECL1 and to be critical for the conformation of CCR5 (34). Mutations which substantially affected the binding of TAK-779 and SCH-C to CCR5 were as follows: Y37A, Y108A, and E283A for TAK-779 and Y37A, WKNF190del, I198A, and E283A for SCH-C. It is noteworthy that the number of mutations that affected the binding of AVC was notably greater than those of TAK-779 and SCH-C. Thus, the CCR5 binding modes of AVC, TAK-779, and SCH-C apparently share some similar features but also have some distinct differences.

Structural analysis locates aplaviroc in the interface of ECL and TM domains – In the present study, a three-dimensional model of human CCR5-CCR5 inhibitor complex was defined by combining the results of site-directed mutagenesis-based analyses (Table 1) and molecular modeling that involved structure refinement and simultaneous docking of inhibitors to an initial structure of CCR5 based on the crystal structure of bovine rhodopsin (23). Fig. 2 illustrates the three-dimensional model of CCR5 that has a seven trans-membrane helical structure. Six hydrophobic cavities were identified in the extracellular, transmembrane, and intracellular domains of CCR5. Among them, a hydrophobic cavity to which CCR5 inhibitors highly likely to bind was identified based on its size and location (red arrow head in Fig. 2). This cavity is the largest one among the six that can accommodate a molecule of the size of AVC and other CCR5 inhibitors and is in the region implicated to have the greatest effect on K_D values with amino acid substitutions introduced in CCR5 among the six hydrophobic cavities identified. It should be noted, however, that the conformations of CCR5 without an inhibitor and CCR5 with the inhibitor can be substantially different from each other, since significant conformational changes would be expected to follow ligand binding to CCR5. Nevertheless, it is intriguing to note that this largest cavity corresponds to the binding site for the retinal ligand in bovine rhodopsin; given the propensity of this pocket to bind fairly large ligands such as the CCR5 inhibitors, it is possible that this binding cavity could accommodate some as-yet uncharacterized ligands produced in the body during the normal function of CCR5, potentially even some with regulatory roles.

Based on the set of the K_D values of AVC in relation to various mutant CCR5 species overexpressed on CHO cells (Table 1), structural analysis of AVC-CCR5 interactions was conducted, which suggested that a series of intramolecular and intermolecular hydrogen bonds occur, which should stabilize the CCR5-AVC complex. We identified a significant network of hydrogen bonds among four amino acid residues: Gly163, Ser180, Lys191, and Thr195 (Fig. 3*A*). Gly163 is located in TM4, Ser180 in ECL2, and Lys191 and Thr195 in TM5. Another network of hydrogen bonds was identified among another four amino acid residues: Tyr37, Glu283, Met287, and Tyr108 (Fig. 3*B*). Tyr37 is located in TM1, Tyr108 in TM3, and Glu283 and Met287 in TM7. These hydrogen bond networks spanning multiple domains appear to maintain the optimal shape of the cavity for the binding of AVC. Indeed, further analysis of the cavity also revealed that the ECL regions have some hydrophilic character (Fig. 4*A*, red arrow head), whereas the rest of the cavity is mostly lipophilic (Fig. 4*A*). The carboxyl and hydroxymethyl of AVC interact with the hydrophilic regions of CCR5. The rest of AVC interacts with the lipophilic region of CCR5 (Fig. 4*A-B*). It is of note that AVC has a molecular weight of 614.2, larger than TAK-779 (Mr. 531.1) and SCH-C (Mr. 557.5), has a substantial hydrophobic contact and fits well inside the large binding cavity within CCR5 as shown in Fig. 4*A*. AVC also forms hydrogen bonds with Cys178, Ser180, Lys191 and Thr195 (Fig. 3*A-B*). It is presumed that these interactions with residues in

multiple ECLs and the interface of extracellular and transmembrane domains are responsible for the tight binding of AVC to CCR5.

Amino acid substitutions are likely to cause substantial conformational changes in ECLs - Substitutions of amino acid residues, which are involved in hydrogen bonding, appear to directly and indirectly disrupt the hydrogen bond networks observed (Fig. 3*A-B*). For example, Gly163, located in TM 4, does not interact directly with AVC, but is responsible for maintaining the shape of the binding cavity by its hydrogen bond interactions with Ser180 and Lys191 (Fig. 3*A*). Thus, the shape of the cavity is most likely altered with G163R substitution, and thereby AVC could lose critical interactions with ECL2 and TM5. In contrast, it was found that G163R exerts minimal effects on the binding of either SCH-C or TAK-779 to CCR5 (Table 1), potentially because these two inhibitors do not have direct hydrogen bond interactions with the ECL or ECL-TM interface.

As mentioned above, the carboxyl of AVC forms hydrogen bonds with Lys191 and Ser180 (Fig. 3*A*). The loss of binding with K191A substitution (Table 1) is likely due to the loss of the hydrogen bond with AVC as well as the altered shape of the cavity, which was confirmed by structural analysis of $CCR5_{K191A}$-AVC complex. Neither SCH-C nor TAK-779 forms hydrogen bonds with Lys191 (Fig. 5*A-B* and Fig. 6*A*), hence it is thought that K191A substitution does not significantly affect the binding affinity of SCH-C or TAK-779 (Table 1). Ile198 located in TM5 has hydrophobic interactions with AVC (Fig. 3*C*). SCH-C and TAK-779 were predicted to have hydrogen bond interactions with Tyr37 located in TM1 (Fig. 5*A-B* and Fig. 6*A-B*), while there appear to be no such interactions with AVC (Fig. 3*B*). This is consistent with the observation that the Y37A substitution drastically changed the binding affinity of SCH-C and TAK-779 to CCR5 (Table 1). Ile198 forms a hydrophobic contact with SCH-C (Fig. 5*C*) although not much with TAK-779, which well explains the reason I198A reduces the K_D value of SCH-C with CCR5 but not that of TAK-779 with CCR5 (Table 1). It is also of note that AVC has direct interactions with residues in the extracellular domain and its proximity (Cys178, Ser180, and Lys191)(Fig. 3*A-B*), which should strongly affect the conformation of extracellular loops in comparison to SCH-C and TAK-779, both of which failed to directly interact with the amino acid residues in the extracellular domain. The interaction of HIV-1-gp120 with ECLs is thought to be critical for the establishment of infection, therefore, one can assume that the binding of AVC to CCR5 should result in a significant loss of interactions with gp120, which could explain the significantly greater effect of AVC in blocking viral infectivity, compared to SCH-C and TAK-779.

Thus, the data above suggest the binding pockets are in the same general area within CCR5, however, the binding interactions of the three inhibitors with CCR5 residues substantially differ from each other, in particular between AVC and other two inhibitors.

Interactions between CCR5 inhibitors in relation to their binding to CCR5 - All three CCR5 inhibitors examined in this study possess the properties of allosteric antagonists of CCR5, while AVC exerts only partial inhibition of the binding to CCR5 and physiological function of ^{125}I-RANTES in comparison to TAK-779 and SCH-C (11). Moreover, although the binding pocket for these inhibitors are all located in the same hydrophobic cavity within CCR5, their binding profiles substantially differ from each other as discussed above. Therefore, we analyzed the interactions of the three inhibitors in relation to $CCR5_{WT}$. When $CCR5_{WT}$-CHO cells were exposed to ^{3}H-AVC (3 nM) for 15 minutes, followed by the addition of various concentrations (1 nM - 10 μM) of unlabelled SCH-C, ^{3}H-AVC binding to CCR5 was reduced only moderately, by up to 32% (Fig. 7*A*). When the interaction between ^{3}H-AVC and unlabelled TAK-779 (0.625 μM – 62.5 μM) was examined, ^{3}H-AVC binding to CCR5 was not significantly replaced by unlabelled TAK-779 (Fig. 7*B*). On the contrary, when ^{3}H-SCH-C was added first and then unlabelled AVC was added, the binding of ^{3}H-SCH-C to $CCR5_{WT}$-CHO cells was significantly blocked (Fig. 7*C*). These data suggest that AVC effectively replaces ^{3}H-SCH-C and binds to $CCR5_{WT}$. The binding of ^{3}H-TAK-779 was likewise blocked by the addition of unlabelled AVC, although the extent of replacement by AVC was lesser as compared to the case of ^{3}H-SCH-C (Fig. 7*D*).

Role of CCR5's amino acid residues with which aplaviroc is associated in HIV-1 infection and CC-chemokine binding - In an attempt to define the biological and virological roles of amino acid residues, with which AVC is associated in this binding to CCR5, we selected 15 mutant CCR5-overexpressing CHO cells and examined profiles of sCD4/gp120 binding and CC-chemokine (RANTES, MIP-1α, and MIP-1β) binding profile. Nine of the 15 mutants were chosen based on the following reasons. Tyr108 was chosen since Tyr108 is within the aromatic cluster seen in the proximity of TM2 and TM3 and is reported to play a crucial role in the CC-chemokine-elicited activation of CCR5 (35). Y37A and E283A were chosen since Tyr37 and Glu283 are involved in the binding of the three inhibitors to CCR5 and have been shown to be highly conserved in CC-chemokine receptors including CCR5, CCR2B, CCR3, CCR1, and CCR4 (6). Five more mutants (G163R, C178A, K191A, I198A, Y251A, and M287E) were also chosen, with which AVC's binding affinity was significantly reduced compared to $CCR5_{WT}$-expressing cells (>5-fold K_D difference)(Table 1). As shown in Fig. 8*A*, all the 9 mutations described above decreased the sCD4/gp120 binding to CCR5 compared to that to $CCR5_{WT}$. It was noted that Y108A, Y251A, and E283A substitutions resulted in the greatest reduction of sCD4/gp120 binding.

We further determined the binding profiles of ^{125}I-RANTES, ^{125}I-MIP-1α, and ^{125}I-MIP-1β to the above 9 mutant CCR5-overexpressing CHO cell lines (Fig. 8*B*). In several CHO cell lines, the CC-chemokine binding profile notably differed from the HIV-gp120/sCD4 complex binding profile. While both K191A and I198A substitutions caused moderate reduction in HIV-gp120/sCD4 complex binding (Fig. 8*A*), CC-chemokine binding was fairly preserved in $CCR5_{I198A}$-expressing cells while CC-chemokine binding was almost completely reduced in $CCR5_{K191A}$-expressing cells. The G163R substitution preserved HIV-gp120/sCD4 complex binding by 34%, however, CC-chemokine binding was substantially spared by 68 – 83%.

We also employed six additional mutant CCR5-overexpressing CHO cells, which showed insignificant to minimal changes (less than 3-fold differences) in their K_D values compared to K_D value for wild-type CCR5 (Table 1). Two substitutions in the extracellular domain of CCR5, D11A (NH_2-terminus) and KE171AA (ECL2), induced substantial reduction in HIV-gp120/sCD4 complex binding by 65 and 70%, respectively. The F112L, F112Y (both in TM3), S180T (ECL2) and M287A (TM7) substitutions caused no significant changes in K_D values (Table 1) or HIV-gp120/sCD4 complex binding (Fig 8*A*). These data suggest that amino acid residues in the proximity of the hydrophobic cavity for AVC that do not change K_D values generally do not affect the HIV-gp120/sCD4 complex binding to CCR5. These 6 substitutions, however, caused CC-chemokine binding inhibition at various degrees, suggesting that the profile of HIV-gp120/sCD4 complex binding to CCR5 differs from that of CC-chemokine binding to CCR5.

We finally generated seven clonal populations of $CD4^+$U373-MAGI cells expressing CCR5 with an amino acid substitution which caused significant reduction in the K_D values of either of the three CCR5 inhibitors and examined their susceptibility to HIV-1_{BaL} infection (Fig. 8*C*). HIV-1_{BaL} effectively infected $CCR5_{WT}$-expressing cells, however, the susceptibility to HIV-1_{BaL} infection was greatly reduced in $CCR5_{Y37A}$-, $CCR5_{Y108A}$-, and $CCR5_{I198A}$-expressing cells and that in $CCR5_{G163R}$-, $CCR5_{C178A}$-, $CCR5_{K191A}$-, and $CCR5_{E283A}$-expressing cells was more greatly limited. These data indicate that the mutations examined in this experiment effectively blocked HIV-1_{BaL} infection, although such mutations, in particular three mutations (G163R, K191A, and I198A), allowed some degrees of sCD4/gp120 binding to $CCR5^+$ cells (Fig. 8*A*).

As noted above, the CC-chemokine binding profile notably differed from the profile of HIV-1_{BaL} infection susceptibility in $CCR5_{G163R}$- and $CCR5_{I198A}$-expressing cells. Moreover, moderate levels of chemokine binding were seen in $CCR5_{Y108A}$- and $CCR5_{E283A}$-expressing cells, while the least infection occurred in these cells. It should be of note that when we examined what ensued upon the binding of RANTES to $CCR5_{G163R}$-expressing cells, it was found that the level of Ca^{2+} flux that occurred in those cells was comparable to that in $CCR5_{WT}$-expressing cells

following stimulation with RANTES (K Maeda *et al.*, unpublished data).

These data, taken together, suggest that the binding affinity of AVC seen with CCR5 variants generally paralleled the HIV-gp120/sCD4 complex binding affinity to mutant CCR5s, although it is of note that further fine-tuned analysis with greater numbers of CCR5 mutants is required for full understanding of the interactions among HIV-gp120/sCD4 complex, CC-chemokines, and CCR5 inhibitors. The data also suggest that certain conformational changes caused by amino acid substitutions (*e.g.*, at Tyr108, Gly163, or Ile198 residues of CCR5) might substantially reduce HIV-1 infection without significantly affecting physiological CC-chemokine-CCR5 interactions.

DISCUSSION

In the present study, we examined the structural and molecular interactions between CCR5 and three CCR5 inhibitors, aplaviroc (AVC), SCH-C and TAK-779. When we exploited site-directed mutagenesis by generating a panel of mutant CCR5-expressing cells, and determined the K_D values of each CCR5 inhibitor with each mutant CCR5 species, the K_D values compiled corroborated our previous results obtained using the mAb replacement assay (11). We found that the binding affinity of AVC to wild-type CCR5 ($CCR5_{WT}$) was the greatest with a K_D value of 2.9 nM as compared to SCH-C and TAK-779 with K_D values of 16.0 and 30.2, respectively (Table 1). It was also noted that the number of mutations that affected the binding of AVC was greater than in the cases of TAK-779 and SCH-C (Table 1). Moreover, the amino acid substitutions with which AVC turned out to have different K_D values were mostly located in the second extracellular loop (ECL2) and its interface with TM 4 (Gly163), or TM5 (Lys191). By contrast, with regard to SCH-C and TAK-779, no substantially different K_D values were obtained with amino acid substitutions in ECL2 (Table 1). The data suggest that not only the binding interactions but also the molecular size and/or bulkiness of AVC are related to the different numbers of K_D-affecting mutations and different profile of K_D values obtained and that AVC forms substantial hydrophobic contacts with and fits well inside the hydrophobic cavity within CCR5 (Fig. 4*A*). It was also thought that such tight interactions of AVC with residues in ECLs and the interface of extracellular and transmembrane domains of CCR5 are responsible for the greater binding affinity of AVC to CCR5 as compared to other two inhibitors.

It was intriguing that certain amino acids such as Gly163 and Lys191 formed critical hydrogen bond networks in the interaction of AVC and CCR5 (Fig. 3*A-B*). It was thought, therefore, that the amino acid substitutions in such positions dramatically altered the binding affinity of AVC to CCR5. It is also noteworthy that Cys178 of ECL2 is presumed to form a putative disulfide bridge with Cys101 of ECL1 and to be critical for the conformation of CCR5 (34). In the present study, C178A substitution, which should disrupt the putative disulfide bridge and cause significant conformational changes in both ECL1 and ECL2, nullified the CCR5 binding affinity of AVC, but not of SCH-C or TAK-779 (Table 1). In this respect, the lesser interactions of SCH-C and TAK-779 with extracellular domains (Table 1) are likely responsible for the lack of influence of the C178A substitution on the binding affinity of SCH-C and TAK-779, corroborating the notion that mutations in ECL2 did not alter the binding of SCH-C and TAK-779 to CCR5 (Table 1).

Two events are likely involved in the reduced binding of inhibitors to CCR5 with an amino acid substitution(s): i) the alteration of direct interaction, if present, between the amino acid residue and the inhibitor and/or ii) an allosteric effect(s) in which there is a significant conformational change(s) of CCR5 either near or distant from the mutated residue. In this respect, in the present work, we have shown multiple hydrogen bond networks are important for the binding of AVC to CCR5 (Fig. 3*A-B*). Some residues such as K191 directly interact with AVC, and hence mutations that lose this direct interaction are very likely responsible for the loss of binding. The lack of drastic changes in the binding of SCH-C and TAK-779, which are not predicted to directly interact with K191, also supports this inference. G163, however, does not directly bind to AVC but is a critical part of the G163-S180-K191-T195 hydrogen network (Fig. 3*A*). Our molecular modeling, however, indicates that arginine at position 163 does not form

hydrogen bonds with S180 or K191. This alteration in the hydrogen bond network probably changes the shape of the cavity in the ECL2-TM4-TM5 region (an allosteric effect near the mutated residue) and results in reduced binding of AVC to $CCR5_{G163R}$. Mutation at residue 283 might be an example of the one causing an allosteric conformational change(s) distant from the mutated residue. Only AVC is predicted to directly interact with E283, but a E283A mutation results in significant loss of binding for all three inhibitors examined. Thus, it is thought that certain amino acid substitutions reduce the binding of an inhibitor even though they are not directly interacting with the inhibitor. It is also of note that mutations at certain residues directly interacting with an inhibitor do not always cause significant loss of binding if CCR5 does not undergo a conformational change(s) or takes an alternate conformation that is not unfavorable for inhibitor binding.

Since a crystal structure of CCR5 is not available, unlike other targets for intervention of HIV infection including HIV reverse transcriptase (36), in the present study, in an attempt to conduct structural analyses of the interactions of CCR5 inhibitors with various mutant CCR5 species, an initial structural model of CCR5 was generated using homology modeling based on the crystal structure of bovine rhodopsin (23). The present approach of combining the site-directed mutagenesis-based data (Table 1) and molecular modeling should be a valuable strategy for gaining structural insights for membrane-bound proteins for which X-ray crystal structures are not as yet available. The CCR5-inhibitor complex structures were defined by iterative optimization of CCR5 and inhibitor structures. Mutated CCR5 structures were also defined and optimized based on the wild type CCR5 structure, and minimized structures of various CCR5 mutants were used as starting structures for obtaining docked complexes of mutated CCR5 with inhibitors. It is of note that in the present study, our modeling study was combined and fine-tuned with the results of the saturation binding assay using a panel of mutant CCR5-expressing cells and tritiated CCR5 inhibitors and the resultant configuration and orientation of inhibitors docked within the hydrophobic cavity of CCR5 yielded a consistent analysis of the structure-activity data. The conformations of CCR5 without an inhibitor and CCR5 bound to an inhibitor are likely to be substantially different from each other since conformational changes are expected to occur upon inhibitor binding to CCR5. Thus, the conformational flexibility of both inhibitors and CCR species were taken into account in our analysis. In this regard, our ongoing analyses of binding affinity profiles using different ^{3}H-labeled CCR5 inhibitors and an expanded panel of mutant CCR5-expressing cell lines should further illuminate the intramolecular and intermolecular interactions of CCR5 and CCR5 inhibitors.

We also examined the binding profile of CCR5 inhibitors when one inhibitor was added to CCR5-overexpressing cells, followed by the addition of the second inhibitor (Fig. 7). Interestingly, when AVC first bound to CCR5 and SCH-C or TAK-779 was subsequently added, both SCH-C and TAK-779 only partially displaced AVC (Fig. 7*A-B*). However, when SCH-C or TAK-779 first bound to CCR5 and AVC was subsequently added, SCH-C and TAK-779 were substantially displaced by AVC (Fig. 7*C-D*). This ineffective displacement of AVC once bound to $CCR5_{WT}$ by SCH-C and TAK-779 could be explained by the difference of their K_D values (2.9 nM for AVC, 16 nM for SCH-C, and 30.2 nM for TAK-779 as illustrated in Table 1). However, it is of note that both SCH-C and TAK-779 failed to displace AVC even with very high concentrations: 3,333-fold (10 μM; Fig. 7*A*) and 20,833-fold (62.5 μM; Fig. 7*B*), respectively, greater than the ^{3}H-AVC concentration (3 nM). Thus, only the difference in K_D values among the three inhibitors unlikely fully explains the failure of AVC replacement by SCH-C and TAK-779. In this regard, a possible explanation is that AVC induces a series of significant conformational changes in CCR5 and, upon the completion of its stable lodging within the hydrophobic cavity within $CCR5_{WT}$, the binding and/or entry into CCR5 of the second inhibitor is hindered and the interaction between AVC and the second inhibitor added is no longer merely competitive. Although the data of displacement experiments using two CCR5 inhibitors discussed above may not offer clear mechanistic explanation at present due to the limitation of the currently available methodologies, the data may have a clinical relevance in the future since more than one

CCR5 inhibitors may be simultaneously administered when multiple CCR5 inhibitors are introduced in the therapy of AIDS. It is also noteworthy that the tight CCR5 binding profile of AVC is presumably related to the extensive and prolonged CCR5 occupancy observed in phytohemagglutinin-activated peripheral blood mononuclear cells ($T_{1/2}$ ~9 hr) (12) and in circulating lymphocytes in HIV-1-negative and HIV-1-positive individuals ($T_{1/2}$ of 69-152 hr depending on different AVC doses), a potentially favorable feature which could enable once daily (*QD*) or twice daily (*BID*) administration of AVC.

In the present study, we observed that amino acid mutations within the transmembrane domains such as Y108A, G163R, and I198A exerted only minimal or moderate effects on the binding of CC-chemokines to CCR5 (Fig. 8*B*), while they caused a substantial reduction in HIV-1 gp120/CD4 complex binding to CCR5 (Fig. 8*A*) and a more drastic reduction in the susceptibility to HIV-1 infection (Fig. 8*C*). It is possible that the molecular size of gp120/sCD4 complex is far greater and its interactions with CCR5 are more extensive compared to the case of CC-chemokines, and therefore, the process for establishing HIV-1 infection is more extensively affected by such amino acid substitutions in comparison to CCR5 binding of CC-chemokines and the ensuing signal transduction. In this regard, a large body of literature has shown that CCR5 regions to which HIV-1's envelope glycoproteins bind are functionally and structurally quite different from those to which CC-chemokines bind (19-21,32,33). Wu *et al.* and Lee *et al.* demonstrated that a group of CCR5's NH_2-terminus-specific monoclonal antibodies did not block the binding of or Ca^{2+} flux induction by CC-chemokines, although ECL2-specific monoclonal antibodies effectively block the binding of CC-chemokines and their Ca^{2+} flux induction (20,21). Navenot *et al.* subsequently confirmed these notions and further demonstrated that a CCR5 chimera with the NH_2-terminus of CXCR2 bound MIP-1α with an affinity similar to that of $CCR5_{WT}$ (33). In contrast, both NH_2-terminus- and ECL2-specific mAbs reportedly blocked efficiently the binding of gp120 to CCR5 although the latter mAbs caused superior inhibition (20,21). These previously published data strongly suggest that the interactions of CCR5 with HIV-1-glycoproteins involve multiple CCR5 domains and consist of more complex processes while those with CC-chemokines involve fewer CCR5 domains and potentially fewer processes. Thus, this implies that the intervention of HIV-1 infection without interrupting physiological CC-chemokine/CCR5 interactions should be feasible. Indeed, AVC does not potently block the physiologic CC-chemokine/CCR5 interactions, although it highly efficiently suppresses the infection of HIV-1 with IC_{50} values of subnanomolar concentrations (11).

Taken together, mutations associated with AVC binding to CCR5 decreased gp120 binding to CCR5 and the susceptibility to HIV-1 infection, while mutations in TM4 and TM5 that also decreased gp120 binding and HIV-1 infectivity had less effects on the binding of CC-chemokines, suggesting that CCR5 inhibition targeting appropriate regions might render the inhibition highly HIV-1-specific, preserving the CC chemokine-CCR5 interactions. The present data should not only help design more potent and HIV-1-specific CCR5 inhibitors, but also should give new insights into the dynamics of CC-chemokine-CCR5 interactions and the mechanisms of CCR5 involvement in the process of cellular entry of HIV-1.

REFERENCES

1. Fauci, A. S. (2003) *Nat Med* 9(7), 839-843
2. Mitsuya, H., and Erickson, J. (1999) Discovery and development of antiretroviral therapeutics for HIV infection. In: Merigan, T. C., Bartlet, J. G., and Bolognesi, D. (eds). *Textbook of AIDS Medicine*, Williams & Wilkins, Baltimore
3. Siliciano, J. D., Kajdas, J., Finzi, D., Quinn, T. C., Chadwick, K., Margolick, J. B., Kovacs, C., Gange, S. J., and Siliciano, R. F. (2003) *Nat Med* 9(6), 727-728

4. Richman, D. D. (2001) *Nature* **410**(6831), 995-1001
5. Department of Health and Human Services (DHHS). (2005) Guidelines for the Use of Antiretroviral Agents in HIV-1-Infected Adults and Adolescents.
6. Raport, C. J., Gosling, J., Schweickart, V. L., Gray, P. W., and Charo, I. F. (1996) *J Biol Chem* **271**(29), 17161-17166
7. Alkhatib, G., Combadiere, C., Broder, C. C., Feng, Y., Kennedy, P. E., Murphy, P. M., and Berger, E. A. (1996) *Science* **272**(5270), 1955-1958
8. Deng, H., Liu, R., Ellmeier, W., Choe, S., Unutmaz, D., Burkhart, M., Di Marzio, P., Marmon, S., Sutton, R. E., Hill, C. M., Davis, C. B., Peiper, S. C., Schall, T. J., Littman, D. R., and Landau, N. R. (1996) *Nature* **381**(6584), 661-666
9. Trkola, A., Dragic, T., Arthos, J., Binley, J. M., Olson, W. C., Allaway, G. P., Cheng-Mayer, C., Robinson, J., Maddon, P. J., and Moore, J. P. (1996) *Nature* **384**(6605), 184-187.
10. Wu, L., Gerard, N. P., Wyatt, R., Choe, H., Parolin, C., Ruffing, N., Borsetti, A., Cardoso, A. A., Desjardin, E., Newman, W., Gerard, C., and Sodroski, J. (1996) *Nature* **384**(6605), 179-183.
11. Maeda, K., Nakata, H., Koh, Y., Miyakawa, T., Ogata, H., Takaoka, Y., Shibayama, S., Sagawa, K., Fukushima, D., Moravek, J., Koyanagi, Y., and Mitsuya, H. (2004) *J Virol* **78**(16), 8654-8662
12. Nakata, H., Maeda, K., Miyakawa, T., Shibayama, S., Matsuo, M., Takaoka, Y., Ito, M., Koyanagi, Y., and Mitsuya, H. (2005) *J Virol* **79**(4), 2087-2096
13. Baba, M., Nishimura, O., Kanzaki, N., Okamoto, M., Sawada, H., Iizawa, Y., Shiraishi, M., Aramaki, Y., Okonogi, K., Ogawa, Y., Meguro, K., and Fujino, M. (1999) *Proc Natl Acad Sci U S A* **96**(10), 5698-5703
14. Strizki, J. M., Xu, S., Wagner, N. E., Wojcik, L., Liu, J., Hou, Y., Endres, M., Palani, A., Shapiro, S., Clader, J. W., Greenlee, W. J., Tagat, J. R., McCombie, S., Cox, K., Fawzi, A. B., Chou, C. C., Pugliese-Sivo, C., Davies, L., Moreno, M. E., Ho, D. D., Trkola, A., Stoddart, C. A., Moore, J. P., Reyes, G. R., and Baroudy, B. M. (2001) *Proc Natl Acad Sci U S A* **98**(22), 12718-12723.
15. Gribble, G. W. (1975) *JCS Chem. Comm.*, 535-541
16. Evans, E. A. (1974) Tritium and its compounds. In., J. Willey and Sons, New York
17. Maeda, K., Yoshimura, K., Shibayama, S., Habashita, H., Tada, H., Sagawa, K., Miyakawa, T., Aoki, M., Fukushima, D., and Mitsuya, H. (2001) *J Biol Chem* **276**(37), 35194-35200.
18. Maeda, Y., Foda, M., Matsushita, S., and Harada, S. (2000) *J Virol* **74**(4), 1787-1793
19. Siciliano, S. J., Kuhmann, S. E., Weng, Y., Madani, N., Springer, M. S., Lineberger, J. E., Danzeisen, R., Miller, M. D., Kavanaugh, M. P., DeMartino, J. A., and Kabat, D. (1999) *J Biol Chem* **274**(4), 1905-1913.
20. Wu, L., LaRosa, G., Kassam, N., Gordon, C. J., Heath, H., Ruffing, N., Chen, H., Humblias, J., Samson, M., Parmentier, M., Moore, J. P., and Mackay, C. R. (1997) *J Exp Med* **186**(8), 1373-1381
21. Lee, B., Sharron, M., Blanpain, C., Doranz, B. J., Vakili, J., Setoh, P., Berg, E., Liu, G., Guy, H. R., Durell, S. R., Parmentier, M., Chang, C. N., Price, K., Tsang, M., and Doms, R. W. (1999) *J Biol Chem* **274**(14), 9617-9626
22. Maeda, Y., Venzon, D. J., and Mitsuya, H. (1998) *J Infect Dis* **177**(5), 1207-1213.
23. Palczewski, K., Kumasaka, T., Hori, T., Behnke, C. A., Motoshima, H., Fox, B. A., Le Trong, I., Teller, D. C., Okada, T., Stenkamp, R. E., Yamamoto, M., and Miyano, M. (2000) *Science* **289**(5480), 739-745.
24. Halgren, T. A., Murphy, R. B., Friesner, R. A., Beard, H. S., Frye, L. L., Pollard, W. T., and Banks, J. L. (2004) *J Med Chem* **47**(7), 1750-1759
25. Xiang, Z., and Honig, B. (2001) *J Mol Biol* **311**(2), 421-430
26. Kaminski, G. A., Friesner, R. A., Tirado-Rives, J., and Jorgensen, W. J. (2001) *J. Phys. Chem. B* **105**, 6474-6487
27. Friesner, R. A., Banks, J. L., Murphy, R. B., Halgren, T. A., Klicic, J. J., Mainz, D. T., Repasky, M. P., Knoll, E. H., Shelley, M., Perry, J. K., Shaw, D. E., Francis, P., and Shenkin, P. S. (2004) *J Med Chem* **47**(7), 1739-1749
28. Exner, T. E., Keil, M., Moeckel, G., and Brickmann, J. (1998) *J. Mol. Model.* **4**, 340-343

29. Viswanadhan, V. N., Ghose, A. K., Revankar, G. R., and Robins, R. K. (1989) *J. Chem. Inf. Comput. Sci.* **29**, 163-172
30. Dragic, T., Trkola, A., Thompson, D. A., Cormier, E. G., Kajumo, F. A., Maxwell, E., Lin, S. W., Ying, W., Smith, S. O., Sakmar, T. P., and Moore, J. P. (2000) *Proc Natl Acad Sci U S A* **97**(10), 5639-5644
31. Tsamis, F., Gavrilov, S., Kajumo, F., Seibert, C., Kuhmann, S., Ketas, T., Trkola, A., Palani, A., Clader, J. W., Tagat, J. R., McCombie, S., Baroudy, B., Moore, J. P., Sakmar, T. P., and Dragic, T. (2003) *J Virol* **77**(9), 5201-5208
32. Dragic, T., Trkola, A., Lin, S. W., Nagashima, K. A., Kajumo, F., Zhao, L., Olson, W. C., Wu, L., Mackay, C. R., Allaway, G. P., Sakmar, T. P., Moore, J. P., and Maddon, P. J. (1998) *J Virol* **72**(1), 279-285.
33. Navenot, J. M., Wang, Z. X., Trent, J. O., Murray, J. L., Hu, Q. X., DeLeeuw, L., Moore, P. S., Chang, Y., and Peiper, S. C. (2001) *J Mol Biol* **313**(5), 1181-1193.
34. Blanpain, C., Lee, B., Vakili, J., Doranz, B. J., Govaerts, C., Migeotte, I., Sharron, M., Dupriez, V., Vassart, G., Doms, R. W., and Parmentier, M. (1999) *J Biol Chem* **274**(27), 18902-18908
35. Govaerts, C., Bondue, A., Springael, J. Y., Olivella, M., Deupi, X., Le Poul, E., Wodak, S. J., Parmentier, M., Pardo, L., and Blanpain, C. (2003) *J Biol Chem* **278**(3), 1892-1903
36. Sarafianos, S. G., Das, K., Hughes, S. H., and Arnold, E. (2004) *Curr Opin Struct Biol* **14**(6), 716-730

ACKNOWLEDGEMENTS

The authors thank Steve LaFon, James Demarest, Alphonso Nillas, Larry Boone, Yashuhiro Koh, Yosuke Maeda, and Philip Yin for helpful discussion and/or critical reading of the manuscript. The authors also thank the Center for Information Technology, National Institutes of Health, for providing computational resources. This work was supported in part by the Intramural Research Program of Center for Cancer Research, National Cancer Institute, National Institutes of Health and in part by a Grant-in-aid for Scientific Research (Priority Areas) from the Ministry of Education, Culture, Sports, Science, and Technology of Japan (Monbu-Kagakusho), a Grant for Promotion of AIDS Research from the Ministry of Health, Welfare, and Labor of Japan (Kosei Rohdosho: H15-AIDS-001), and the Grant to the Cooperative Research Project on Clinical and Epidemiological Studies of Emerging and Re-emerging Infectious Diseases (Renkei Jigyo: No. 78, Kumamoto University) of Monbu-Kagakusho.

FIGURE LEGENDS

Fig. 1. Structures of aplaviroc (AVC), TAK-779, and SCH-C.

Fig. 2. Hydrophobic cavities identified within CCR5. Six hydrophobic cavities are identified within human CCR5, defined using MOLCAD (Sybyl 7.0). Note the largest hydrophobic cavity (red arrow head) that is likely to accommodate a molecule of the size of AVC and other CCR5 inhibitors and is in the region implicated to have greatest effects on K_D values (see mutagenesis-based results in Table 1).

Fig. 3. Hydrogen bond networks within CCR5 critical for AVC binding to CCR5. The structure of CCR5-AVC complex was defined with iterative structural refinement using docking and homology modeling. Only polar hydrogen atoms are shown. Panel *A*, An intramolecular hydrogen bond network comprised of Gly163, Ser180, Lys191, and Thr195 is seen. Gly163 is located in TM4, Ser180 in ECL2, and Lys191 and Thr195 in TM5. The structural analyses illustrate the presence of intermolecular hydrogen bonds of AVC with residues Cys178, Ser180, Lys191, and Thr195 of CCR5. Panel *B*, An intramolecular hydrogen bond network is seen involving Tyr37, Glu283, Met287, and Tyr108. Tyr37 is located in TM1, Tyr108 in TM3, and Glu283 and Met287 in TM7. Glu283 forms hydrogen bond interactions with the hydroxymethyl of AVC. Intramolecular hydrogen bonds are shown in pink, and the intermolecular hydrogen bonds in green. Note that the hydrogen bond networks spanning multiple domains should maintain the optimal shape of the cavity for the binding of AVC (Fig. 4*A-B*). Panel *C*, The predicted van der Waals contact between AVC and CCR5 residues Lys191 and Ile198. AVC is shown in green spheres, whereas Lys191 and Ile198 in magenta.

Fig. 4. The configuration of aplaviroc within CCR5. Panel *A*, AVC lodged within the binding cavity of CCR5. The CCR5 cavity was defined with its lipophilic potential using MOLCAD. The region near the extracellular domain has some hydrophilic character (red arrow head), whereas the rest of the cavity is mostly lipophilic. The carboxyl and hydroxymethyl of AVC interact with the hydrophilic regions of CCR5, whereas the rest of AVC interacts with the lipophilic regions of CCR5. Panel *B*, A docked structure of AVC (tube representation) bound to CCR5, illustrating the relative location of AVC within CCR5. Important binding site residues of CCR5 are shown in wires. Polar hydrogens are only shown. Note that TM 1, 2, and 3 are towards the viewer from the plane and TM 6 and 7 are away from the viewer behind the plane.

Fig. 5. Interactions of SCH-C with CCR5 residues. Panel *A*, The configuration of SCH-C (shown in CPK) obtained with mutagenesis-based data (Table 1) combined with structural analyses. CCR5 residue orientations (shown in tubes) vary from that in Fig. 4 since conformational flexibility of receptors during docking of each inhibitor was taken into account. Panel *B*, Tyr37 forms hydrogen bonding interactions with SCH-C, and hence Y37A mutation reduces the binding affinity of SCH-C with CCR5. Note the location of Tyr108 and compare its corresponding location for the complex with TAK-779. SCH-C is shown in tubes and CCR5 residues in wires. Only polar hydrogens are shown in panel *A* and *B*. The molecules are colored by atom types (carbon, grey; oxygen, red; nitrogen, blue; hydrogen, cyan; sulfur, yellow; bromine, green). Panel *C*, van der Waals interactions of SCH-C (green) with Lys191 and Ile198 (magenta). There is tight hydrophobic binding of SCH-C with Ile198. Unlike AVC, Lys191 does not form significant interactions with SCH-C.

Fig. 6. Interactions of TAK-779 with CCR5 residues. Panel *A*, The configuration of TAK-779 within the CCR5 binding pocket. Panel *B*, Tyr37 forms a hydrogen bonding interaction with TAK-779. Note the orientation of Tyr108 in comparison to CCR5's complex with SCH-C. Tyr108 forms π-π and hydrogen bond interactions with TAK-779 and represents a critical residue in agreement with the mutagenesis-based results (Table 1). Only polar hydrogens are shown. The molecules are colored by atom types (carbon, grey; oxygen, red; nitrogen, blue; hydrogen, cyan; sulfur, yellow).

Fig. 7. Interactions between CCR5 inhibitors in relation to CCR5. $CCR5_{WT}$-CHO cells were exposed to ^{3}H-AVC (3 nM; panel *A* and *B*), ^{3}H-SCH-C (3 nM; panel *C*), or ^{3}H-TAK-779 (10 nM; panel *D*), for 15 min, followed by the exposure to various concentrations (from 1 nM to 62.5 μM) of unlabelled SCH-C (panel *A*), TAK-779 (panel *B*), or AVC (panel *C* and *D*) for 30 min. The cells were then thoroughly washed, lysed, and the radioactivity of the lysates was counted. All experiments were performed in duplicate and the data shown are mean values ± SD. The amounts of ^{3}H-CCR5 inhibitor bound to the cells are shown as mean % control values (each control value was obtained without an indicated unlabelled CCR5 inhibitor).

Fig. 8. Effects of amino acid substitutions in CCR5 on sCD4/gp120 binding, HIV infection, and CC-chemokine binding. Panel *A*, Profiles of the binding of $sCD4/gp120_{YU2}$ complex to various $CCR5_{MT}$ species overexpressing CHO cells. All values were normalized with the CCR5 expression level of each $CCR5_{MT}$ compared to that of $CCR5_{WT}$ (See Experimental Procedures). Panel *B*, Profiles of the binding of ^{125}I-RANTES, ^{125}I-MIP-1α, and ^{125}I-MIP-1β to various $CCR5_{MT}$-expressing CHO cell preparations. All values were normalized with the CCR5 expression level of each $CCR5_{MT}$ compared to that of $CCR5_{WT}$. All assays were performed in duplicate or triplicate. Panel *C*, The susceptibility of various $CCR5_{MT}$-overexpressing U373-MAGI cells. For testing each of $CCR5_{MT}$-overexpressing cell preparations, multiple clones were examined. In each set of experiments, $CCR5_{WT}$-clone #1 (solid column) served as a standard (100%).

Table 1. Binding affinity of CCR5 inhibitors to mutant CCR5s

Mutant CCR5 overexpressed on CHO cells		K_D value[a] (nM) Aplaviroc	SCH-C	TAK-779	gp120/sCD4 binding[b] (%control)
wild type		2.9 ± 1.0	16.0 ± 1.5	30.2 ± 7.6	100 ± 13.3
D11A	*NH_2- terminus*	3.0 ± 0.6	12.4 ± 2.0	24.5 ± 3.7	35.4 ± 4.7
Y37A	*TM1*	7.9 ± 0.9	**>200**	**98.9 ± 11.5**	35.4 ± 3.7
Y108A		**19.8 ± 4.4**[c]	11.8 ± 1.1	**>200**	13.2 ± 1.0
F112L		4.0 ± 2.6	30.0 ± 6.4	33.0 ± 7.2	
F112Y	*TM3*	6.8 ± 1.1	35.8 ± 7.6	28.5 ± 3.1	111 ± 6.9
F113A		**13.3 ± 2.3**	43.8 ± 6.3	32.7 ± 3.3	
F113Y		8.6 ± 3.4	45.3 ± 12.1	32.4 ± 3.0	
G163A	*TM4-ECL2*	8.0 ± 4.2	25.0 ± 8.2	24.0 ± 5.9	
G163R		**>200**	46.3 ± 16.5	88.3 ± 22.9	34.1 ± 5.4
R168A		**13.2 ± 3.3**	21.0 ± 8.1	43.0 ± 4.7	
KE171AA		2.8 ± 0.1	34.8 ± 6.8	30.5 ± 0.7	29.6 ± 2.2
C178A		**>200**	27.1 ± 4.4	34.5 ± 3.5	20.9 ± 1.0
S180A		5.7 ± 1.2	31.8 ± 14.4	18.2 ± 3.2	
S180T	*ECL2*	1.5 ± 0.6	25.4 ± 6.8	41.0 ± 3.8	101 ± 15.0
S180E		**13.9 ± 1.7**	16.5 ± 2.2	25.0 ± 3.5	51.6 ± 1.1
YS184AA		2.0 ± 0.8	21.3 ± 5.0	28.0 ± 2.5	
YSQY184AAA		2.0 ± 0.6	14.9 ± 0.6	32.3 ± 5.8	
QY186AA		2.8 ± 0.5	14.7 ± 8.8	35.2 ± 5.8	
Q188A		6.6 ± 1.4	23.8 ± 1.5	37.9 ± 2.5	
WKNF190del		**>200**	**49.2 ± 1.7**	80.1 ± 16.7	
K191A		**>200**	26.5 ± 7.1	35.0 ± 3.8	45.7 ± 0.6
K191R	*ECL2-TM5*	**9.0 ± 5.6**	34.1 ± 19.1	47.1 ± 8.8	
K191N		**14.2 ± 1.1**	35.8 ± 9.2	35.1 ±9.3	
K197A	*TM5*	**9.2 ± 4.3**	16.8 ± 2.9	14.7 ± 1.1	
I198A		**24.6 ± 4.8**	**52.4 ± 3.0**	54.9 ± 6.9	51.7 ± 3.0
Y251A	*TM6*	**36.5 ± 9.5**	21.5 ± 8.6	43.0 ± 4.5	14.5 ± 0.7
E283A		**>200**	**>200**	**>200**	4.3 ± 0.6
M287A	*TM7*	6.8 ± 2.3	28.0 ± 9.1	39.8 ± 7.5	104 ± 3.9
M287E		**14.8 ± 1.7**	32.2 ± 4.2	53.1 ± 3.7	22.0 ± 0.8

[a] K_D values were determined using saturation binding assays (Experimental Procedures).

[b] gp120/sCD4 binding affinity to $CCR5_{MT}$ is shown by % control (see Experimental Procedures for reference), the data is also shown in Figure 8*A*

[c] K_D values more than 3-fold compared to that with $CCR5_{WT}$ are shown in bold. All K_D values were determined on multiple occasions (twice to 6 times). Considering the standard deviation for the wild-type, and other mutations, a 3-fold difference was seen to be statistically significant.

Figure 1

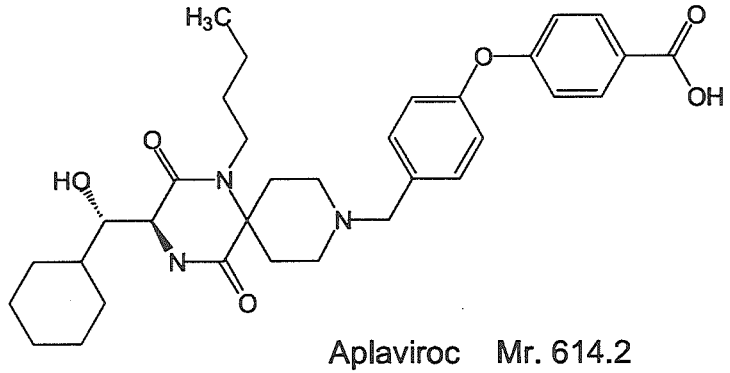

Aplaviroc Mr. 614.2

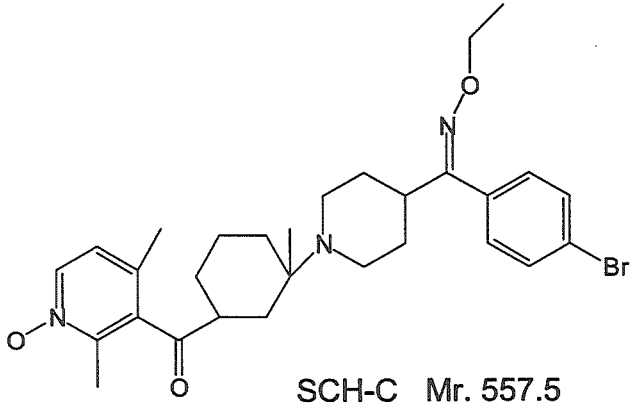

SCH-C Mr. 557.5

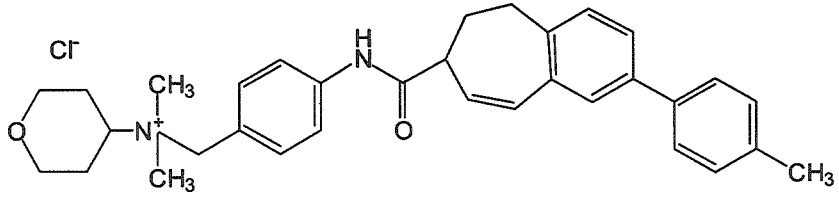

TAK-779 Mr. 531.1

Figure 2

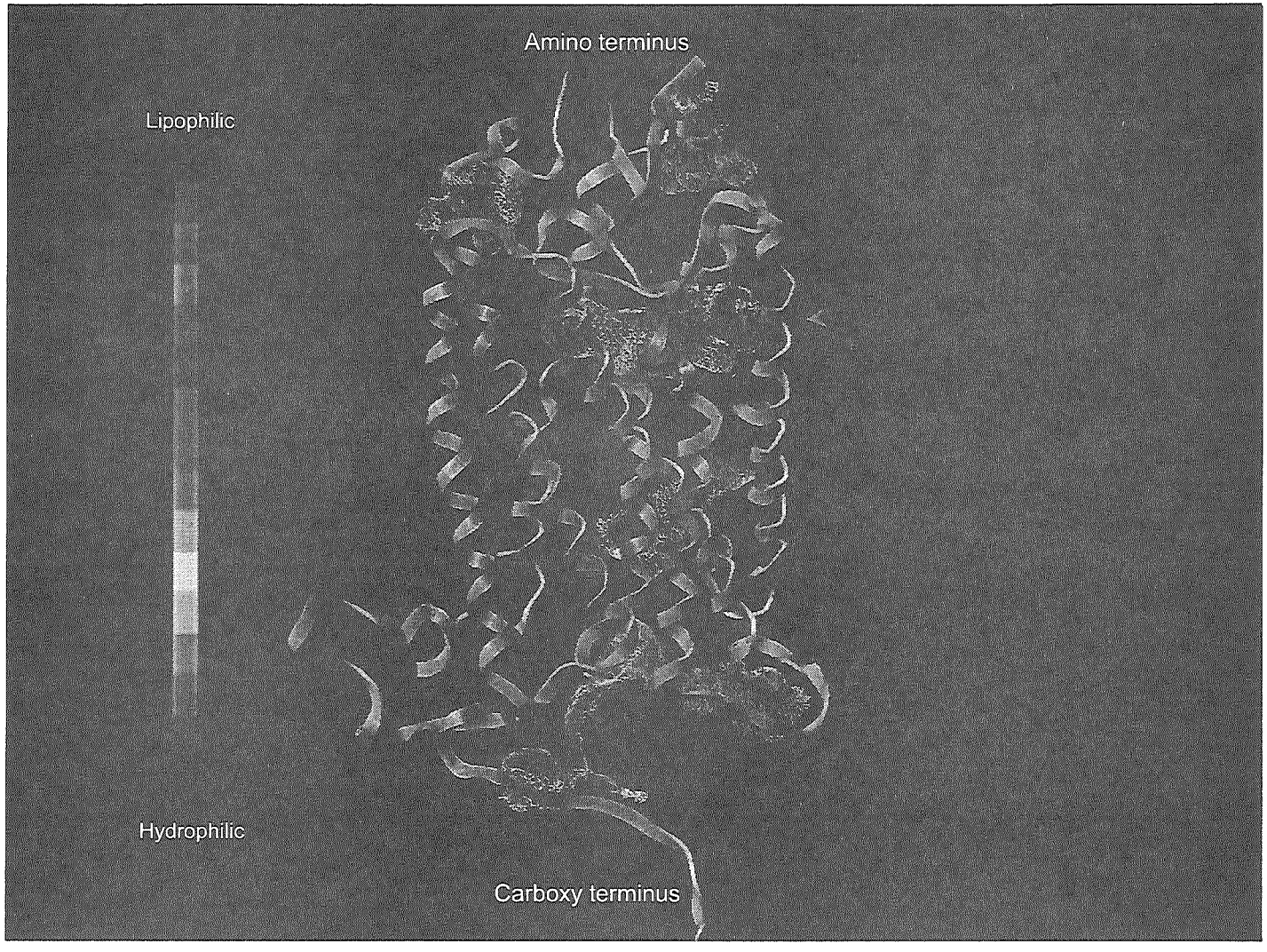

Figure 3

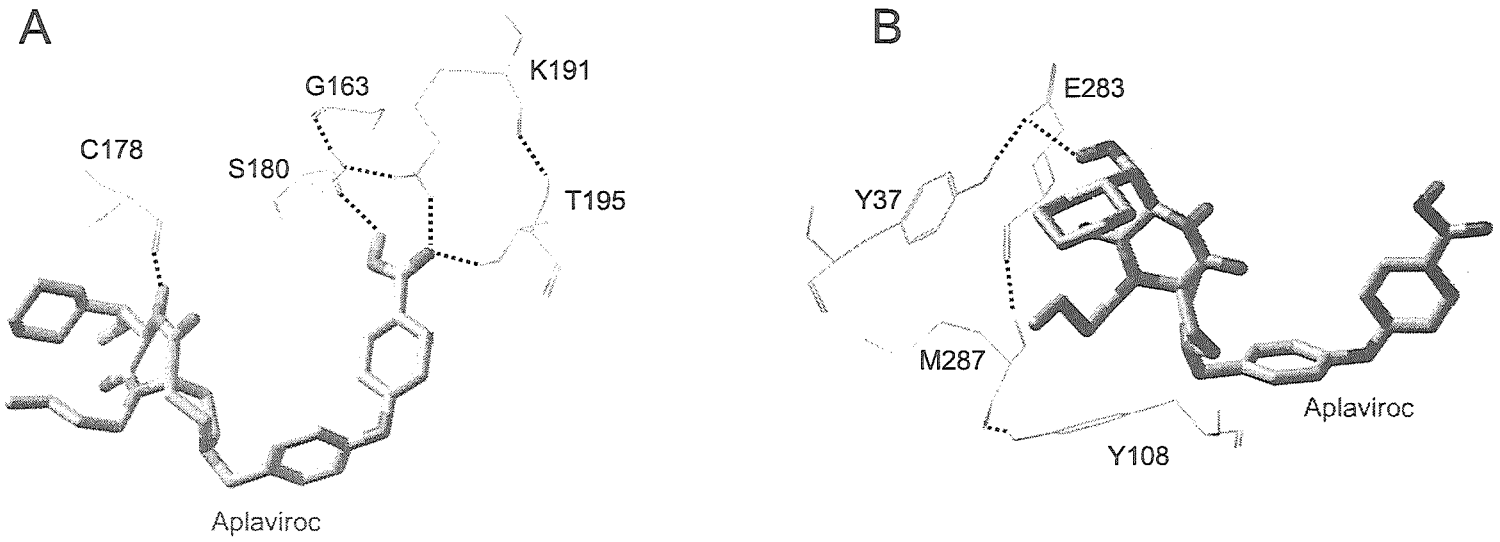
A
G163
K191
C178
S180
T195
Aplaviroc
B
E283
Y37
M287
Aplaviroc
Y108

Figure 3